Biogeochemistry **35:** 447–470, 1996.

A biogeochemical model for chalk alteration by fungi in semiarid environments

ERIC P. VERRECCHIA[1] & JEAN-LOUIS DUMONT[2]
[1]*U.M.R. 5561 C.N.R.S., Centre des Sciences de la Terre, Université de Bourgogne, 6 Bd Gabriel, 21000 Dijon, France. E-mail: EVERRECC@SATIE.U-BOURGOGNE.FR;* [2]*E.R. 109 C.N.R.S., Géomorphologie et transferts de surface, 24 rue des Tilleuls,14000 Caen, France*

Received 13 June 1996; accepted 18 June 1996

Key words: biomineralization, calcium oxalate, calcium carbonate, calcrete, fungi, model

Abstract. Fungal filaments are the most abundant organic features in weathered profiles developed on chalky limestone ("platy calcrete"). Their activity affects the mineral dynamics of the pore/carbonate microsystem. A theoretical biogeochemical model is proposed to describe the Ca-oxalate-carbonate cycle related to fungal activity in dry environments.

The system studied is the pore itself (defined as the reactor) delimited by its wall and its content: solutions, gases (air and CO_2), microorganic material, their transformation products and the minerals present (calcite and calcium oxalate). The system exchanges gas and solution with the outside environment, which includes micritic calcite, solutions, a gaseous phase (air and CO_2), and the nanoporosity of the pore wall constituted by the micritic matrix. A diagram of pH = f(log $|Ca^{2+}|$) is constructed to simulate the behaviour of various fungal excretions, whether the system is open or semi-closed. Two steps are studied. In the first step, the fungi is in full metabolic activity, and assumed to secrete i) an organic diacid (BH_2) of soluble calcium salt, or ii) oxalic acid, or iii) soluble sodium oxalate, or iv) CO_2. In the second step, bacteria transform the oxalates into carbonates. In the first step, the model concurs with petrographic observations, on the condition that the system is semi-closed and the aggressive agent produced by the hypha is mostly oxalic acid $(COOH)_2$. In the second step, the pore solution becomes saturated in calcite, whether the system is open or semi-closed. This explains the calcium carbonate precipitation inside the pore as needles or microsparite and impregnation of the micritic matrix around the pores. In conclusion, the presence of fungi allows a redistribution of calcium carbonate. This secondary cementation is strong in the case of recrystallization of pore walls and weaker when infilling voids with needles.

Abbreviations:

K_i = equilibrium constant
pX = cologarithm of compound X diassociation / equilibrium constant
π_i = solubility product
A = $|C_2O_4^{2-}|$, concentration of oxalate ions
C = $|Ca^{2+}|$, concentration of calcium ions
C_T = total dissolved carbon in $mol.l^{-1}$

$|M^+|$ = total concentration (in equivalents per litre) of cations other than Ca^{2+} in carbonated solutions (heterocationic)

$|B^-|$ = total concentration (in equivalents per litre) of anions other than carbonates in carbonated solutions (heteroanionic)

ε = difference between cations other than Ca^{2+} and anions other than CO_3^{2-}

k_H = $38.3.10^{-3}$ $mol.l^{-1}.atm^{-1}$ at 20 °C. Henry's Law constant: ratio of solubility ($|CO_2|$) to vapor pressure (pCO_2); therefore, the partition of the CO_2 between air and water

K_w = $|H^+|.|OH^-|$; water diassociation constant

Δ denotes a difference.

aq denotes "aqueous".

Introduction

Weathered profiles developed on chalky parent rocks in arid zones commonly include a layer called a "platy caliche/calcrete" or "platy zone" (Moore 1989). The platy zone, located just below the laminar crust, is characterized by: 1) a micritic matrix with an alveolar texture, 2) needle-fiber crystals (in the form of random or banded cement in voids), and, 3) the most abundant organic feature, mineralized fungal filaments (Krumbein 1968; Esteban & Klappa 1983). In regard to its genesis, several problems are posed by the complex relationships between needle-fiber calcite precipitation, the formation of calcium oxalate crystals, evolution of the porosity, and the influence of fungal colonies. The points that remain unclear are:

1) The incongruity of the porosity, strength, and $CaCO_3$ content: although platy calcrete has a porosity between 20 and 40%, its strength is relatively high, between 120 and 220 kg/cm^2 and its $CaCO_3$ content is higher than the overlying and underlying horizons (Gile 1961; Yaalon & Singer 1974; Esteban & Klappa 1983; Verrecchia 1992).
2) The origin of the needle-fiber crystals: these have long been identified as low-magnesium calcite, but their origin (physico-chemical or biogenic) is still controversial (see synthesis in Verrecchia & Verrecchia 1994).
3) The nature of mineralized filaments: commonly considered as calcified filaments (e.g. Kahle 1977; Klappa 1979; Phillips et al. 1987; Wright 1989; Monger et al. 1991), they have also been identified as fungal filaments encrusted with calcium oxalate (e.g. Graustein et al. 1977; Cromack et al. 1979; Arnott & Webb 1983; Horner et al. 1983; Verrecchia et al. 1993). Although the transformation of calcium oxalate into calcium

carbonate crystals is known to take place (Cromack et al. 1979; Verrecchia et al. 1993), the chemical consequences for the platy calcrete fabric are not well understood.

The aim of this paper is to propose a theoretical biogeochemical model of the Ca-oxalate-carbonate cycle related to fungal activity and to compare it with observations supplemented by chemical and mineralogical data from weathered chalk profiles in semiarid environments. Based on this model, a two-step scenario is proposed to explain the origin of the platy calcrete fabric and features.

Properties of fungi reviewed

It is worthwhile to start with a review of filamentous fungi because they are a critical factor in the development of the model. Filamentous fungi belong to heterotrophic and saprophytic organisms and are agents in the degradation of organic material in soils. Mycelian hyphae constitute all the filamentous and ramified parts of the fungi's thallus. The diameter of these filaments varies from 1–2μm to 5–10μm. Four main biochemical characteristics of fungi (Callot et al. 1985) will be used to construct the model: i) the hyphae possess a skeletal wall or membrane, which is initially made of pectin and then later incorporates cellulose; ii) absorption and excretion of substances can take place through all parts of the hyphal wall; iii) Ca^{2+} can accumulate in the thallus, preferentially in or on the membranes; and iv) filamentous fungi accumulate and then excrete large quantities of organic acids, in particular oxalic acid. Oxalic acid has an important role in the chemical activity of fungi, in that it constitutes "the first oxidation product resulting from the aerobic breakdown of carbohydrate found to accumulate in fungus culture" (Foster 1949). Excreted by the hypha in limestones or environments abundant in calcium carbonate, the acid can react with the $CaCO_3$ (Webley et al. 1963; Robert & Berthelin 1986) to form calcium oxalates (whewellite or weddellite), minerals found in lichens (Wadsten & Moberg 1985), discomycetes (Horner et al. 1983) and ectomycorhizes (Cromack et al. 1979; Malajczuk & Cromack 1982; Lapeyrie et al. 1990). Identification of oxalic acid and calcium oxalate in lichens on calcareous rocks is not recent (Braconnot 1825).

In the past few years, the morphology, the structure, and the consequence of production of these minerals (calcium oxalates) have been the object of many studies. They have shown that the crystalline forms of calcium oxalates vary from sharp needles (raphides) to flat or polypyramidal crystals (Franceschi & Horner 1980; Frey-Wyssling 1981; Verrecchia et al. 1993). The production of these minerals is directly related to the presence of organic material (Leavens 1968), which play a fundamental role in the calcium, iron, and aluminum

cycles in surficial environments (Graustein et al. 1977; Cromack et al 1977; de la Torre et al. 1993; Johnston & Vestal 1993). In calcareous rocks, filamentous fungi are fairly abundant and are irregularly distributed in the micropores of the rock, thus modifying the petrographic structure.

Petrographical description of fungi and associated minerals in chalk pores

Before developing the biogeochemical model, a brief petrographic description of the material will be presented. Hyphae occupy pores of various dimensions, from several μm to several hundreds of μm. The organization of the microstructure is similar, whether the pore is small and inhabited by one filament or larger and occupied by a colony. For example, in samples of weathered chalk from Galilee, Israel (Verrecchia 1992; Verrecchia et al. 1993) the structure shows a succession of many features surrounding the pore, which is occupied by the fungal colony (Figure 1a and b). The matrix (m in Figure 1a and b) is 90–95% calcium carbonate (micrite). The insoluble residue (using hydrochloric acid as a solvent) is composed of clays, quartz, and feldspars of aeolian origin. The matrix does not show any plasmic segregations, except for organization around voids. In contact with the matrix and towards the centre of the pore (p in Figure 1a and b), microsparitic crystals (q in Figure 1a) grow in the direction of the void. Dark irregular bands cut across these crystals (c in Figure 1a and b), covering the edges of the pores. These bands are composed of clays (clay cutans). Enrichment of clay in the proximity of a pore is indicated by the distribution profile of the aluminum measured using the Energy Dispersive Spectrometry (EDS) microprobe coupled with the Scanning Electron Microscope (SEM; Jaillard 1987). High intensity Al peaks emphasize the presence of clay quasi-coatings (c in Figure 1a). These clays are concentrated over about 40μm inside the matrix, which is partly recrystallized into microsparite. Outside this zone, the amount of Al decreases drastically to a continuous background. These clay accumulations are not related to leaching. They are not oriented and remain isotropic around the edge of the pore, commonly forming quasi-coatings (Figure 1a). The pore space is occupied by filamentous mycelium bodies (f in Figure 1a and b), bristling with crystals in the shape of sharp needles or parallelepipeds of various lengths and widths (Figure 1c and d). The pore is the site of biological activity, where solutions circulate (reacting with the mineral walls) and diffuse back through the matrix micropores. The pore is partly infilled by needle-fiber calcite (n in Figure 1a and b). The micritic matrix around the pore is enriched in $CaCO_3$ and even recrystallized and separated from the pore by a mat of calcite crystals (n and q in Figure 1a).

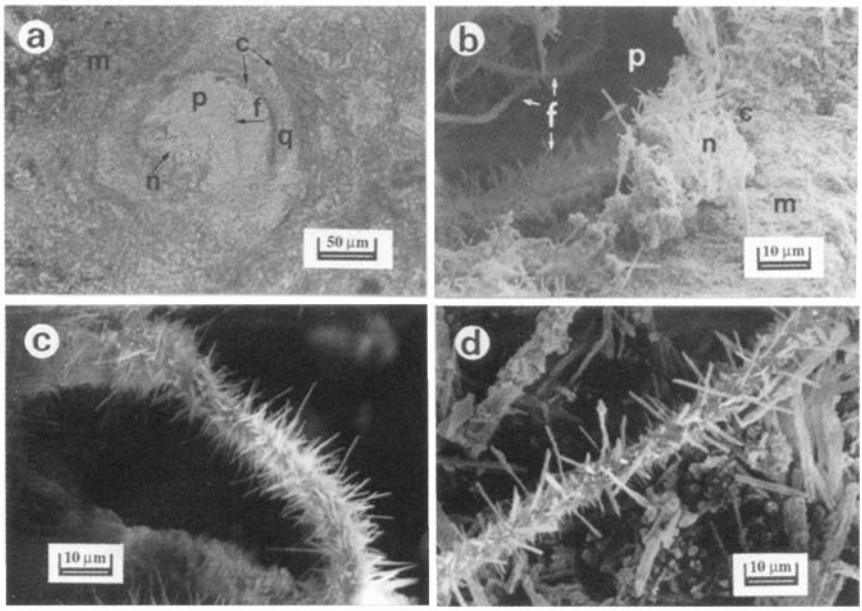

Figure 1. a. View of the pore-fungi-limestone microniche observed under optical microscope in plane polarized light (PPL). Microphotograph shows: the mineralized filament covered by calcium oxalate crystals (f), the pore void (p), needle-fiber calcite (n), black layers composed by clays as quasi-coatings and coatings (c), the bright layer of secondary calcite cement (q), and the micritic matrix (m). *b.* Cross section from center (upper left-hand corner) to periphery (lower right hand corner) of microniche observed under scanning electron microscope. Letters refer to same objects as in c. Three different generations of filaments are visible (f) showing an increasing amount of oxalate needles from youngest to oldest. *c.* Acicular crystals (raphidic- or needle-shaped) of calcium oxalate on fungal filaments in a platy calcrete from Nazareth (Galilee, Israel). SEM micrograph. *d.* Acicular (styloïdic- or columnar-shaped) and prismatic crystals of calcium oxalate on fungal hyphae, same origin as c. See synthesis of calcium oxalate crystal habits in Verrecchia et al. (1993). On the right-hand side, rods of needle-fiber calcite.

Weakly mineralized fungal bodies appear in the form of hollow filaments 2–10 μm in diameter. Their surface is smooth or rough (covered with microspheres 0.3–0.5 μm in diameter). These microspheres were interpreted as bacterial coccoids by Klappa (1979). In other cases, crystalline germs pierce through the membrane, giving the filament a rough appearance (Figure 1b, c and d). Filaments are commonly divided into two branches, the intersections sometimes being a preferred site for crystallizations. Hyphae devoid of crystals are exceptional. In general, mycelia are densely covered by minerals having a large variety of crystal morphologies.

Absence of hyphae in pores results in uneven redistributions of plasma, where clay coatings are uncommon and calcite needles take different forms. Therefore, it is probable that fungal activity affects the mineral dynamics of

the pore/carbonate microsystem. Presence of mycelium alters the appearance of pores and consolidates the periphery of pores by depositing calcite quasi-coatings or coatings (calcitans). In more powdery samples, all stages of colonization appear, from micropores with one filament to macropores filled with numerous colonies. In the latter case, the relationship between pore organization and fungal activity is more obvious.

Model development

Exchange system between the pore and the exterior: hypothesis on the principles of how it functions (Figure 2)

Establishing a model begins with the definition of a system and its modes of functioning, i.e. conditions that are imposed and that can be varied. In conformity with the described microscopic observations, the system will be the pore itself, delimited by its calcitic wall and its content: solutions, gases (air and CO_2), organic material (mycelium, microorganisms), their transformation products, and the minerals present (calcite and calcium oxalate, assumed here to be whewellite). This site will be considered as a reactor (Figure 2) and separated from the non-pore environment with which it exchanges gases and solutions. The outside or non-pore environment consists of micritic calcite, solutions, a gaseous phase (air and CO_2), and the nanoporosity of the pore wall, which is constituted by the micritic matrix. The goal is to examine transformations (dissolution, calcite reprecipitation) that occur after the transfer of solutions from the exterior (non-pore environment) to the system and vice versa (Figure 2). The transfers of gas and solutions between the system and its immediate non-pore environment occur through the pore walls.

Certain assumptions are necessary to explain the exchanges inside the system. First, we consider that the exchange of dissolved substances occurs by diffusion or convection through the pore walls. Convection takes place due to the effect of evapotranspiration produced at the surface of the soil after it has rained. The rate of solution transfer is sufficiently low for equilibrium to be attained between the solid – solution – gas on either side of the pore wall, without necessarily reaching an equilibrium between the pore and the non-pore environment. Second, exchanges between solid, liquid and gas are made under the following conditions: i) because of the large contact surfaces in chalk material, it will be assumed that there is always an equilibrium between $CO_{2\ gas} \leftrightarrow CO_{2\ dissolved}$ at contact surfaces. Therefore, the concentration of $CO_{2\ dissolved}$ in the solution of the system and that of the non-pore or soil surface (denoted as CO_2 from here on) will be characterized by its equilibrium pCO_2; ii) exchange between solid $CaCO_3$ and dissolved carbon-

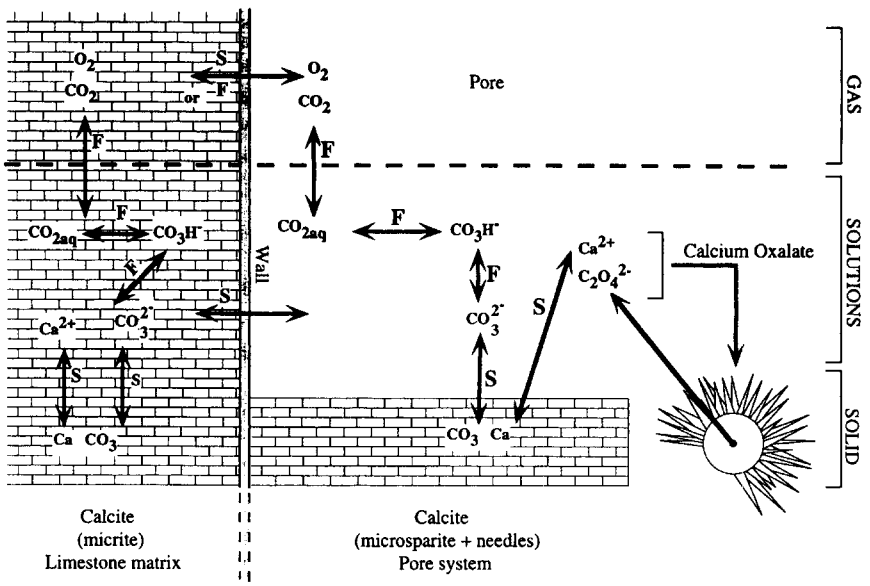

Figure 2. Sketch of the "reactor", consisting of the pore-fungi-calcium carbonate-calcium oxalate microsystem, showing the main chemical reactions. Three phases are present in the pore as well as in the limestone matrix: a solid phase constituted by calcium oxalate crystals and calcite, solutions, and gases, mainly oxygen and carbon dioxide. Regarding the diffusion of molecules in the medium, certain reactions are slow (S), whereas others are fast (F).

ated compounds initiated by diffusion will be considered a slow process; iii) gaseous exchange through the pore wall will be considered in two extreme cases: either the wall is very porous and permits rapid exchange, leading to a $pCO_{2\ \text{system}}$ equal to $pCO_{2\ \text{environment}}$ (defining an "open system"), or the wall is semi-permeable (blocking of pores by intense calcification and/or clay coatings, for example). Therefore, the $pCO_{2\ \text{system}}$ is different from the $pCO_{2\ \text{environment}}$ and equilibrium takes place after an infinitely long time. This case is defined as a "semi-closed system"; iv) finally, it is assumed that only biogeochemical processes initiate phenomena of dissolution and reprecipitation, thus excluding evaporation and dilution.

Modelling of the system using $CO_2 - CaCO_3 - H_2O$ equilibrium diagrams

Our goal is to predict the aggressive or encrusting quality of the solution after its transfer, according to the sequence: outside the system → system → outside the system. This can be accomplished using $CO_2 - CaCO_3 - H_2O$ equilibrium diagrams (Roques 1964; Roques 1975). The construction of the diagram pH = f(log $|Ca^{2+}|$) is adapted to the environment studied (Figure 3). Taking into account the range of pHs used (6.5 to 8.5), $|OH^-|$, $|H^+|$, $|C_2O_4^{2-}|$,

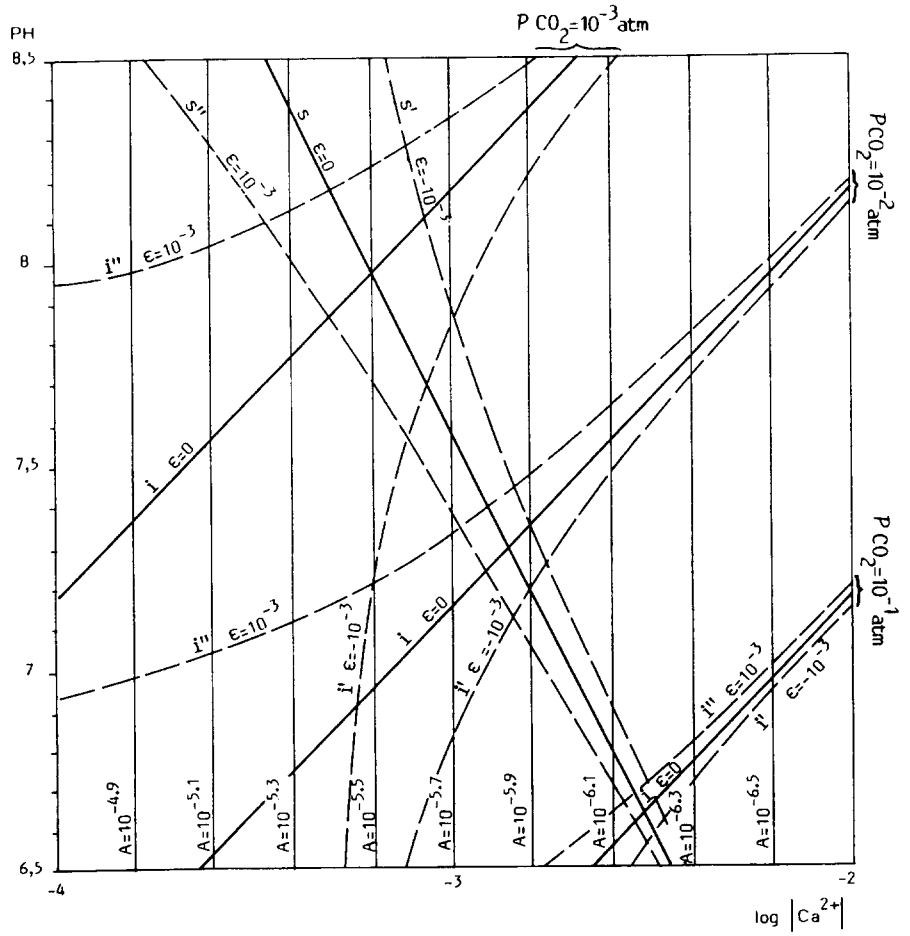

Figure 3. Diagram of saturation curves pH = f(log $|Ca^{2+}|$). Concentrations are given in mol.l^{-1}. The constants used are temperature, T = 20 °C, $pK_1(CO_2)$ = 6.45, $pK_2(CO_3H^-)$ = 10.38, $p\pi_1$(calcite) = 8.53, $p\pi_2$(calcium oxalate) = 8.7, pK_A(oxalic acid) = 1.42, and pK_w(water) = 14. S, s′ and s″ are saturation curves regarding calcite. I, i′ and i″ curves represent the isobars of pCO_2 equilibrium. For $\varepsilon < 0$, read s′ and i′; for $\varepsilon = 0$, read s and i; for $\varepsilon > 0$, read s″ and i″. Vertical lines (A) represent saturation curves regarding whewellite.

and $|CO_3^{2-}|$ are negligible compared to $|Ca^{2+}|$ and $|CO_3H^-|$. Under these conditions, the electrical neutrality of the solution is expressed by:

$$2|Ca^{2+}| + \varepsilon \approx |CO_3H^-| \tag{1}$$

$$\text{where } \varepsilon = |M^+| - |B^-| \tag{2}$$

If $\varepsilon > 0$, heterocations are dominant. If $\varepsilon < 0$, heteroanions are dominant. The dissolution equilibria of $CO_{2\ dissolved}$ (represented by CO_2) are given by:

$$K_1 = \frac{|H^+|.|CO_3H^-|}{|CO_2|} \tag{3}$$

$$K_2 = \frac{|H^+|.|CO_3^{2-}|}{|CO_3H^-|} \tag{4}$$

At the dissolution equilibrium of $CaCO_3$ and CaC_2O_4 (saturation) and at a given temperature, we have:

$$|Ca^{2+}|.|CO_3^{2-}| = \pi_1 \tag{5}$$

$$|Ca^{2+}|.|C_2O_4^{2-}| = \pi_2 \tag{6}$$

The dissolved CO_2 is equilibrated by a partial pressure of equilibrum pCO_2, at a given temperature (Henry's law):

$$|CO_2| = k_H.pCO_2 \tag{7}$$

In the case of saturation regarding calcite, all of the preceding relationships lead to the equation (8):

$$2|Ca^{2+}| + \varepsilon \approx \frac{\pi_1.|H^+|}{|Ca^{2+}|.K_2} \tag{8}$$

In cases of undersaturation and supersaturation, equations (1), (4) and (7) lead to (9):

$$|H^+| = \frac{K_1.k_H.pCO_2}{\varepsilon + 2|Ca^{2+}|} \tag{9}$$

Then, three groups of curves (Figure 3) can be constructed on the graph $pH = f(\log |Ca^{2+}|)$:

- the first group represents calcite and solutions in equilibrium, the pH decreasing with the $|Ca^{2+}|$ (s, s′, s″ curves). These curves are constructed for a given value of ε, which expresses the difference between equivalents in cations other than Ca^{2+} and equivalents in anions other than the carbonate. The branch (s′) is constructed for $\varepsilon < 0$, (s) for $\varepsilon = 0$, and (s″) for $\varepsilon > 0$. Therefore, one branch of the curve delimits two domains: to the left of the curve is the zone of undersaturation in calcite and to the right is that of supersaturation;

- the second group in which pH increases with log $|Ca^{2+}|$ (i, i′, i″ curves) represents the isobars of pCO_2 equilibrium, whether the solution is undersaturated, saturated or supersaturated in calcite. Each group of isobars is sub-divided into branches of curves at a constant ε (branch i′ for $\varepsilon < 0$, i for $\varepsilon = 0$ and i″ for $\varepsilon > 0$). Three values of ε are shown on the diagram (-10^{-3}, 0, $+10^{-3}$). The branches of the curves corresponding to intermediate $|\varepsilon|$ are inserted between $|\varepsilon| = 10^{-3}$ and $|\varepsilon| = 0$;
- the third group is composed of vertical lines of saturation in whewellite, where $A = |C_2O_4^{2-}|$.

In order to simplify the diagram, supplementary limits are necessary. First, the nature of the dissolved components depends upon the exchanges between gas (CO_2 and air), water, and minerals present (calcite and whewellite) of defined solubility. In the system, it is also necessary to consider the acids or organic salts secreted by the hypha. ε will be considered exclusively in the interior of the pore, assuming ε is negligible in the exterior because of the effects of diffusion/dilution. Second, the temperature of the system is taken as 20 °C and activities and concentrations are considered to be interchangeable. Mg^{2+} does not come into the reaction. Complexes will not be taken into account and the exchange capacity will be considered negligible. Third, at the pHs studied, $C_2O_4^{2-}$ is considered as non-hydrolyzed; due to the low solubility of CaC_2O_4, it is assumed that the solutions are always saturated with this mineral and that this only slightly modifies the carbonated species concentrations. Fourth, the limits for the variables in the pH = f(log $|Ca^{2+}|$) diagram (Figure 3) are defined as follows:

- pCO_2 range: the lower limit is the ambient atmosphere or 3.10^{-4} atm. The upper limit is 0.1 atm, which represents a maximum for soils, in general. Laboratory measurements (Foster 1949) have shown that optimum metabolic activity for *Botrytis* took place at 2.10^{-3} atm, a value within the chosen range (according to Foster, this activity is low for a pCO_2 of 3.10^{-4} atm);
- $|Ca^{2+}|$ range: the values used were those of natural waters on carbonate rocks, where $10^{-4} < |Ca^{2+}| < 10^{-2}$ mol.l^{-1};
- pH range: the pH is between 6.5 and 8.5, given the intervals for $|Ca^{2+}|$ and pCO_2.

Three states are defined for the solutions. In state 0, the solution is exterior to the system. This is illustrated by a figurative point on the saturation curve s, at $(pCO_2)_0$. In state 1, the solution has penetrated into the system and reequilibrated. It is represented by a figurative point on the new saturation curve s, s′ or s″ according to the case, at $(pCO_2)_1$. In state 2, the solution has left the system and has once again equilibrated outside the pore. It is represented by a figurative point on the saturation curve s, s′, or s″, according

to the case, at $(pCO_2)_2$. Two cases are considered: either the system is open or semi-closed. If the solution is in equilibrium at an assigned $pCO_2 = (pCO_2)_0$, the system is said to be "open". If the equilibrium partial pressures in CO_2 are different from one part of the wall to the other, the system is called "semi-closed". In this case, the diffusion is extremely weak and pCO_2 inside and outside the system are not equal.

The model evolves in two distinct steps. During the first step, the fungi is in full metabolic activity, the hypha secretes different substances, one of which is oxalic acid. Without precise data on the composition of fungal secretions produced during their metabolism, four possible types of secretions are considered: i) an organic diacid (BH_2) of soluble calcium salt, assumed to be entirely dissociated at the studied pH; ii) oxalic acid; iii) a soluble oxalate (e.g. sodium oxalate), and iv) CO_2. During the second step, the oxalates transform into carbonates under the action of bacteria (Cromack et al. 1977). In order to clarify the processes involved in this transformation, the paths from the initial to the final state will be discussed in detail.

First step: during fungal activity

If the system is semi-closed, four cases can be considered (Figure 4). First (Figure 4a), during BH_2 production ($\varepsilon < 0$), $CaCO_3$ dissolves inside the pore (step $0 \rightarrow 1$), reaches the saturation line s′, and finally reprecipitates outside the pore ($1 \rightarrow 2$). Second (Figure 4b), oxalic acid is excreted. ε is small, due to the weak solubility of CaC_2O_4. This implies that s and s′ are practically interchangeable. During the step $0 \rightarrow 1$, pH and $|Ca^{2+}|$ decrease first, due to the precipitation of CaC_2O_4. The concentration in Ca^{2+} increases again at the expense of the $CaCO_3$, in order to fill the deficit, and reaches the saturation curve s. This results in dissolution inside the pore. In step $1 \rightarrow 2$, the reprecipitation of calcite takes place outside the pore, because of a decrease of pCO_2. Third (Figure 4c), a soluble oxalate salt, such as $Na_2C_2O_4$, is produced by the microorganism. First, CaC_2O_4 precipitates at constant pH. Na^+ being freed at constant pCO_2 ($(pCO_2)_0$), the figurative point reaches the new $(pCO_2)_0$ curve. $CaCO_3$ dissolves to fill the deficit, and point 1 (on the saturation curve s″) is reached. During the step $1 \rightarrow 2$, because of the return to $(pCO_2)_0$, $CaCO_3$ is dissolved outside the pore, in this case. Fourth (Figure 4d), we consider that only CO_2 is excreted, therefore $\varepsilon = 0$. This is followed by dissolution of CO_2 and dissolution of calcium carbonate in the pore to reach s. Reprecipitation occurs outside the pore to reach 0 again.

If the system is open (Figure 5), the pCO_2 is fixed and controlled by the exterior. Therefore, stages 1 and 2 are interchangeable and there is no reprecipitation outside the pore in any of the four cases. Inside the pore

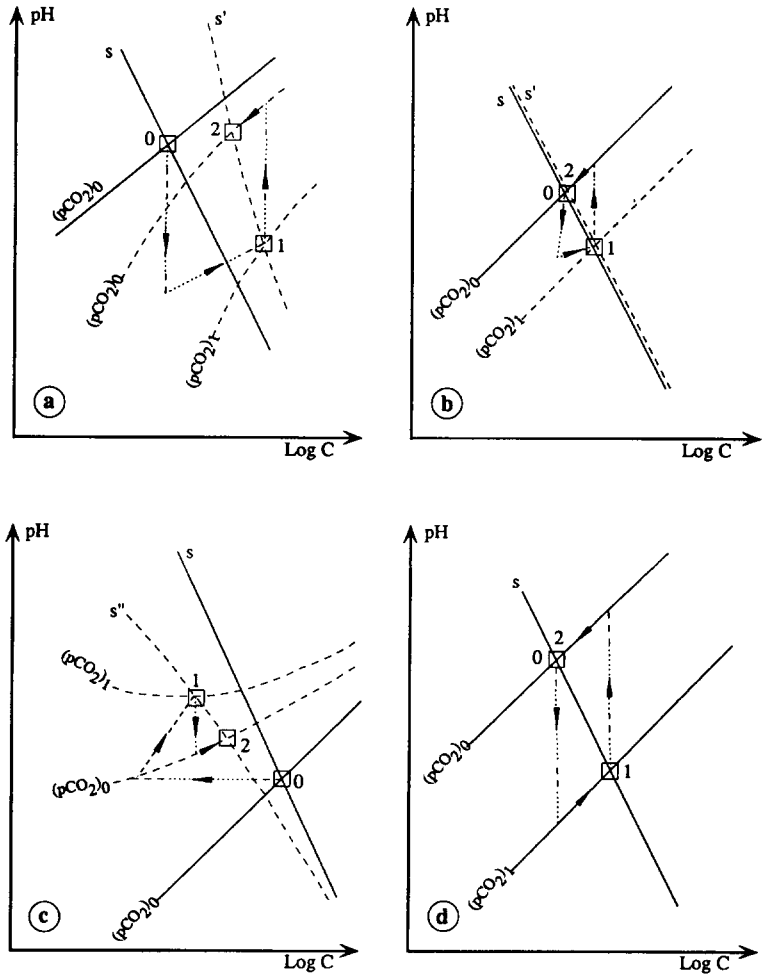

Figure 4. Evolution of reactions when system is semi-closed. The hypha excretes (a) a diacid, (b) oxalic acid, (c) a soluble oxalate salt or (d) carbon dioxide. a. In this case, $\varepsilon < 0$. First, the pH decreases because of acid excretion (vertical branch). Dissolution occurs inside the system, increasing the $|Ca^{2+}|$ in the pore solution (step 0 → 1) until it reaches saturation regarding the pore pCO_2 (point 1 on s′). Then, by diffusion outward or absorption of CO_2 by microorganisms, the pH increases until the curve reaches the equilibrium pCO_2 outside the system, leading to a precipitation of calcium carbonate (step 1 → 2) outside the pore. b. The mechanism is similar to that in a but s and s′ are practically interchangeable because ε is very small. First, calcium oxalate precipitates (vertical branch from 0) and calcium carbonate is partly dissolved until the solution reaches point 1. As in a, in step 1 → 2, calcite precipitates outside the pore. c. In this case, $\varepsilon > 0$ (curve s″). First, oxalate precipitates (horizontal line from 0) followed by calcite dissolution (step 0 → 1) until saturation (point 1). The reequilibrium with the exterior pCO_2 leads to dissolution outside the pore. d. In this case, $\varepsilon = 0$ (s curve). First, the pH decreases because of CO_2 excretion. Calcite is dissolved, increasing the $|Ca^{2+}|$ in the pore solution until the saturation point 1 (step 0 → 1). Then by reequilibrium with the exterior pCO_2, there is reprecipitation of calcite outside the pore (step 1 → 2).

(step 0 → 1), there is dissolution of $CaCO_3$ in the first and third cases (Figure 5a, c). No reaction takes place in the other two cases (Figure 5b, d).

Observations of petrographic structures have revealed precipitated calcium oxalate, corrosions (dissolutions) of the pore wall, clay coatings, and calcite reprecipitations associated with the clay coatings and as secondarily quasi-calcitans cementing the inter-poral areas. These observations concur with the models, under two conditions: the model is a semi-closed system and the aggressive agent produced by the hypha is mostly oxalic acid $(COOH)_2$. The open system option does not explain the $CaCO_3$ reprecipitations. The only aggressive component in the model to act (the only one compatible with the observations) is oxalic acid. If each aggressive agent acted alone, strong acids and carbonic acid would be eliminated because they do not produce calcium oxalate salts. Regarding $Na_2C_2O_4$ acting alone, it cannot result in $CaCO_3$ reprecipitations, but conversely, results in dissolutions.

In conclusion, during a period of fungal activity, the system should be open in order for the fungi to live. Its activity leads to 1) the production of oxalic acid that results in the crystallization of calcium oxalate needles, 2) dissolution of the calcium carbonate pore wall, and 3) formation of clay coatings by decalcification. The evolving system, the clays being stabilized (Foster 1981), and the progressive closure of the wall by infilling, modify the equilibrium. The partial pressures of CO_2 are not the same inside and outside the pore. At this stage, there is dissolution and reprecipitation of calcitans outside the pore.

Second step: transformation of oxalates into carbonates

Calcium oxalate, in its solid or liquid state, can be transformed into calcium carbonate by soil bacteria (Cromack et al. 1977). Two cases are considered in which transformation takes place in a closed or open system, according to the following sequence:

$$C_2O_4^{2-} + \frac{1}{2}\,O_2 + H_2O \rightarrow 2CO_3H^- \qquad (10)$$

$$\downarrow$$

carbonated species

$$\downarrow$$

supersaturation

$$\downarrow$$

$CaCO_3$ precipitation

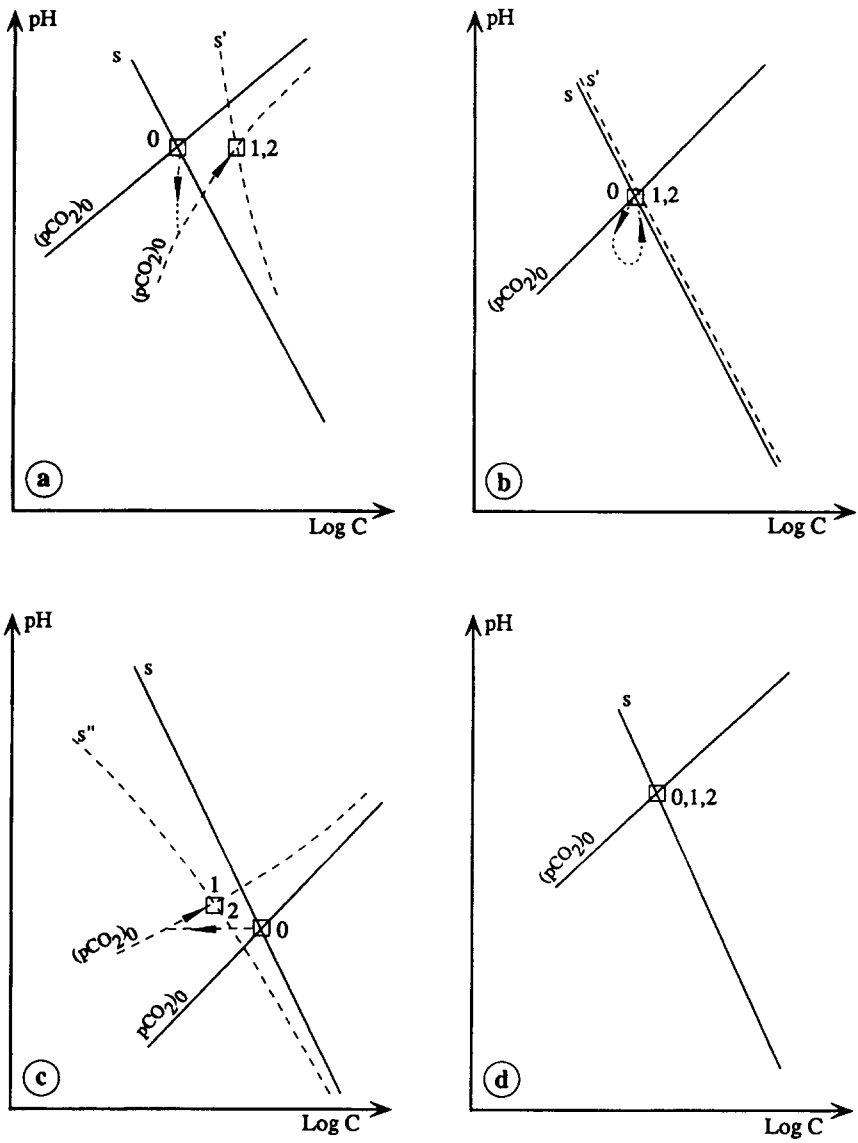

Figure 5. Evolution of the reactions when the system is open. The hypha excretes (a) a diacid, (b) oxalic acid, (c) a soluble oxalate salt or (d) carbon dioxide. a. In this case, $\varepsilon < 0$. First, the pH decreases because of acid excretion (vertical branch from 0). Dissolution occurs inside the system, increasing the $|Ca^{2+}|$ in the pore solution (step $0 \rightarrow 1, 2$) until it reaches saturation curve s'. There is no precipitation outside the pore. b. The mechanism is similar to that in a but s and s' are practically interchangeable because ε is very small. Therefore, no changes occur. c. Precipitation of calcium oxalate occurs inside the system, decreasing the $|Ca^{2+}|$ in the pore solution (step $0 \rightarrow 1, 2$) until it reaches saturation curve s''. There is no precipitation outside the pore. d. All the steps are interchangeable. No reactions occur.

The balance of carbon being dissolved, the carbon inside the solution, and the electric charges have to be considered to explain the variation of pH versus log C, when the system is semi-closed. Because $|CO_3^{2-}|$ and $|CO_2|$ can be neglected at pH <8.3 and pH >8.3 respectively, and at pH = 8.3, $|CO_3^{2-}| = |CO_2|$ (see Appendix), the variation of pH versus log C can be divided into two steps. In step 0 → 1, the pH starts to increase in the supersaturated regions toward a lower pCO_2 (log C increasing by dissolution). In step 1 → 2, the solution precipitates $CaCO_3$: the figurative point comes back on the saturation curve, the pH decreases to reach the final state 2, which has a lower pCO_2 than at state 0 (see Appendix). In conclusion, the global balance shows a depletion in $|Ca^{2+}|$, the pH increases after calcium oxalate has been transformed into carbonated species, which in turn are precipitated in the presence of Ca^{2+} to form $CaCO_3$.

When the system is open, the pCO_2 does not vary. Supersaturation occurs with an increase in pH (step 0 → 1). Precipitation leads to the final state 2, identical to the initial state 0, after a decrease of pH. Therefore, during the period of transformation, the pore solutions become saturated in calcite, whether the system is open or semi-closed. Calcite precipitation can occur either inside the pore or on the pore wall (calcitan). Calcite appears as a microsparitic cement observed with the microscope or precipitates in the matrix microporosity. If crystallization occurs inside the pore, it can take the form of winglet growth along the length of fine needles or occasionally forms polycrystalline calcite needles. If crystallization occurs outside, i.e. in the matrix porosity, it reinforces the calcite cement already deposited during fungal activity. Two cases are possible, according to whether or not $CaCO_3$ precipitation is assisted by a solid support (calcite crystals or biological membranes). If the nucleation is homogeneous, and therefore purely physico-chemical within the pore solution, the initial solution must become supersaturated faster locally than its diffusion toward the wall, followed by cementation. Because of the low concentration in dissolved oxalates compared to the initial calcareous solution, this case is unlikely. If the nucleation at the center of the pore is heterogeneous because of the existence of "biological supports" (e.g. coccimorph or bacillimorph bacteria) or preexisting needle-fibers, then precipitation and crystal shapes can be explained this way. This hypothesis is further reinforced because heterogeneous nucleation necessitates a weaker supersaturation than a homogeneous nucleation (Wollast 1971). Therefore, it is possible that certain calcite needles and/or lateral enrichments form after the transformation from oxalate to carbonate.

Discussion

Results and limitations of the theoretical biochemical model

The proposed biogeochemical model is based on chemical equilibria in the "carbonate-calcium oxalate-water-soil atmosphere-microorganisms" system. It concurs with observations on the following sequence of phenomena taking place in the pore and its periphery: a) fungal activity leads to the production of various acids, including oxalic acid, which react with Ca^{2+} in the solution. This results in the precipitation of crystalline acicular calcium oxalate covering the hyphal walls; b) the subsequent acidity of the solutions leads to a corrosion of the internal pore walls, at the same time as the solution is being enriched in dissolved carbonates. During migration of the solution through the pore wall, $CaCO_3$ can recrystallize in the wall due to a decrease of pCO_2; c) fungal activity precedes biodegradation of the calcium oxalate, which is then transformed into carbonate; d) this results in a precipitation of calcite either in the pore interior (in the form of needles or winglets on preexisting needles) or on the pore periphery; e) cementation at the pore periphery, which occurs during one or another of the steps, tends to progressively close the pore-solution system and cement the sediment, resulting in the hardening of the chalky parent material.

Taking into account our observations and the theoretical model, it is undeniable that organic activity plays an important role in the cementation of chalky material and calcretes in surficial and semiarid environments. The influence of life results in at least two types of late diagenetic cementations. First, microsparites form as cutans or quasi-calcitans around the pores, in the horizons where mycelian activity is high. Second, the cementation is composed of needle-fiber calcite, which can also be of fungal origin, but is undoubtedly related to different species of fungi (Verrecchia & Verrecchia 1994). In the first case, the precipitation of cements results in a greater hardening of the micritic rock. In the second case, the results are more complex. Over a period of time, biogeochemical reactions in the environment lead to a transformation of oxalates into carbonates and to the secondary precipitation of calcium carbonate on the needles or on preexisting nuclei. This supplementary input of calcite only partially contributes to differential hardening of the material and to infilling the pores. In areas where needles are most abundant, pores are partially infilled and, aboveall, the crystals do not form a cohesive cement. This explains why, despite the abundance of secondary calcium carbonate and reprecipitation, the weathered chalk profile stays locally powdery and weakly indurated. Redistribution of calcium carbonate does not necessarily lead to a pronounced hardening. It seems that lowering the porosity need not necessarily be correlated to an increase either in crystal

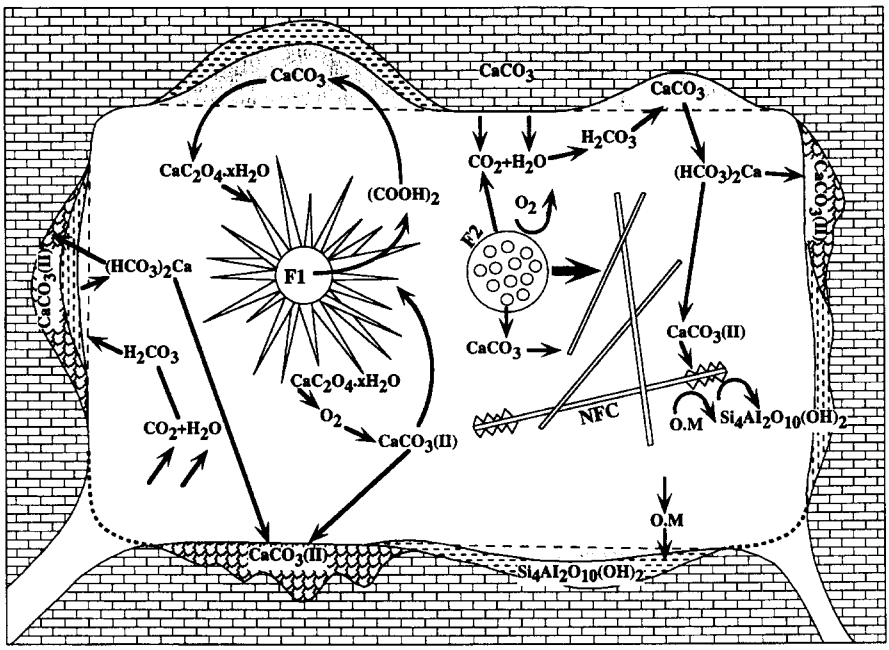

Figure 6. Sketch of chemical compounds and crystals present in the pore-fungi-carbonate-oxalate microsystem. Grey areas represent dissolved limestone around the pore. Areas in dashed lines represent clay coatings and quasi-coatings. The (II) following the calcium carbonate formula $CaCO_3$ refers to a calcium carbonate cement, secondary in origin, and related either to transformation of oxalate into carbonate, or to precipitation from the pore solution. O.M.: organic matter. F1: fungal filament covered by oxalate crystals. F2: mineralized fungal filament containing needle-fiber calcite. After decay of organic matter, needle-fibers (NFC) are freed in pore (thick black arrow). Thick dashed lines denote progressive closing of the system.

size or hardness, contrary to the conclusions of Yaalon & Singer (1974). We showed that an increase in microporosity can be accompanied by abundant secondary precipitation of acicular crystals, micrite or microsparite, which harden only differentially the s-matrix.

Biogeochemical cycle

Figure 6 gives a summary of biogeochemical relationships between the elements present in the pores and the cements, as well as cutans or quasi-cutans. During exposure of chalky rocks to the atmosphere, fungi colonize the pores and develop in the interior of the microporosity by digitation of fine hyphae. During metabolic acitivity, the cellular glucose oxidizes. The fungi produce large quantities of oxalic acid by hydrolysis of oxalo-acetates. This acid is released in its free form into the system (Schlegel 1986). The final balanced reactions are:

$$C_6H_{12}O_6 + 3CaCO_3 + O_2 \rightarrow 2C_2O_4^{2-} + 2CH_3COO^- + 3Ca^{2+} + 3H_2O + CO_2 \quad (11)$$

$$\text{with } C_2O_4^{2-} + Ca^{2+} \rightarrow CaC_2O_4 \quad (12)$$

The presence of fungi induces a mineral neogenesis that destabilizes the local environment by the use of cations and acidification. First, fungal activity leads to the dissolution of the micritic matrix by the secretions of acids and respiration (CO_2). This biodissolution explains the presence of decalcified clays in a hypo-cutan position, as observed by Steinen (1974, p. 1024) who noted "the dense-appearing walls are gray-brown in color". These clays are probably stabilized by polysaccharides derived from organic material (Foster 1981), which inhibit the efficiency of weak leaching in semiarid environments. The precipitation of oxalates is accompanied by the liberation of CO_3^{2-} radicals that, together with those produced by carbonic acid, react with Ca^{2+} resulting in the secondary precipitation of $CaCO_3$, by diffusion into the matrix where the conditions of pH and pCO_2 are more favorable. This would explain the presence of micritic recrystallization rings (microsparite in quasi-calcitans). This process contributes to harden the material by secondary cementation.

Under conditions permitting the proliferation of bacteria when fungi die, oxalate salts transform into calcite by bio-oxidation (Cromack et al. 1977):

$$2CaC_2O_4 + O_2 \rightarrow 2Ca^{2+} + 2CO_3^{2-} + 2CO_2 \quad (13)$$

This additional input of calcite also contributes to infill the pores. In the same environment, other fungi species concentrate the available calcium carbonate and mineralize it. During decomposition of the hypha, calcite needles contained within the sheath are released and constitute (together with the micritic matrix), favored sites of secondary calcite precipitation, resulting in serrated edges on the calcite needles (Verrecchia and Verrecchia 1994).

In conclusion, fungi that have suffered either precipitation of calcium oxalate on their periphery or crystallization of calcite needles in their sheaths, redistribute calcium carbonate leading to a secondary cementation. This cementation is not very efficient when it infills voids with needles, but moreso when it results in quasi-calcitanic mineralization.

Conclusion

The use of equilibrium diagrams allowed the simulation of the evolution of the fungi-calcite-whewellite-solution-gas system in several steps. Fungal activity

and an open porous system lead to i) production of oxalic acid that results in the crystallization of calcium oxalate needles, ii) dissolution of the calcium carbonate pore wall, and iii) formation of clay coatings by decalcification. As the system evolves, it progressively closes and equilibria are modified. Partial pressures of CO_2 are no longer equal on all sides of the pore wall. At this stage, dissolution occurs in the pore and calcite reprecipitates outside the pore system. After the fungi die, there is a transformation of Ca-oxalate into Ca-carbonate by bacteria. During this step, the pore solution becomes saturated in calcite, whether the system is open or semi-closed. Calcite precipitation can occur either inside the pore or on the pore wall. Precipitation of calcite in the matrix micropores will contribute to harden the chalky material, whereas precipitation of calcite needles inside the pores will only increase the $CaCO_3$ content, without contributing to a strong cementation.

In conclusion, presence of fungi in chalk induces a mineral neogenesis that destabilizes the environment using cations and acidification. Fungi are undoubtedly a factor in early lithification, alteration, and diagenesis in terrestrial subsurface limestones. It is already well known that they greatly contribute to extensive weathering of stone monuments (e.g. Krumbein et al. 1989; Danin & Caneva 1990; de la Torre et al. 1993).

Acknowledgements

The authors wish to thank K. E. Verrecchia and V. H. E. Rolko for improving the English version of the text, and A. Bussière (Centre National de la Recherche Scientifique, Dijon) for drafting the figures. Many thanks to Prof. D. Yaalon (Hebrew University of Jerusalem) for reviewing and improving the first version of the text. This paper is a contribution to the research theme *Fonctionnement des systèmes sédimentaires* of the *Unité Mixte de Recherche 5561 du Centre National de la Recherche Scientifique, Paléontologie analytique et géologie sédimentaire* (Dijon, France).

References

Arnott HJ & Webb MA (1983) The structure and formation of calcium oxalate crystal deposits on the hyphae of a wood rot fungus. Scanning Electron Microscope 1983/IV: 1747–1758

Braconnot H (1825) De la présence de l'oxalate de chaux dans le règne minéral; existence du même sel en quantité énorme dans les plantes de la famille des lichens, et moyen avantageux d'en extraire de l'acide oxalique. Ann. Chim. Phys. 28: 318–322

Callot G, Mousain D & Plassard C (1985) Concentrations de carbonate de calcium sur les parois des hyphes mycéliens. Agronomie 5: 143–150

Cromack KJr, Sollins P, Todd RL, Fogel R, Todd AW, Fender WM, Crossley ME & Crossley DA Jr (1977) The role of oxalic acid and bicarbonate in calcium cycling by fungi and

bacteria: Some possible implications for soil animals. Ecol. Bull. (Stockholm) 25: 246–252

Cromack KJr, Sollins P, Graustein WC, Speidel K, Todd AW, Speicher G, Li CY & Todd RL (1979) Calcium oxalate accumulation and soil weathering in mats of the hypogeous fungus Hysterangium crassum. Soil Biol. Biochem. 11: 463–468

Danin A & Caneva G (1990) Deterioration of limestone walls in Jerusalem and marble monuments in Rome caused by cyanobacteria and cyanophilous lichens. Int. Biodeter. 26: 397–417

Esteban M & Klappa CF (1983) Subaerial exposure environment. In: Scholle PA, Bebout DG & Moore CH (Eds) Carbonate Depositional Environments Memoir 33 (pp 24–45). American Association of Petroleum Geologists, Tulsa

Foster JW (1949) Chemical Activities of Fungi. Academic Press, New York

Foster RC (1981) Polysaccharides in soil fabrics. Science 214: 665–667

Franceschi VR & Horner HT (1980) Calcium oxalate crystals in plants. Bot. Rev. 46: 361–427

Frey-Wyssling A (1981) Crystallography of the two hydrates of crystalline calcium oxalate in plants. Amer. J. Bot. 68: 130–141

Gile LH (1961) A classification of Ca horizon in soils of a desert region, Dona Ana County, New Mexico. Soil Sci. Soc. Am. Proceed. 25: 52–61

Graustein WC, Cromack KJr & Sollins P (1977) Calcium oxalate: Occurrence in soils and effects on nutrient and geochemical cycles. Science 198: 1252–1254

Horner HT, Tiffany LH & Cody AM (1983) Formation of calcium oxalate crystals associated with apothecia of the discomycete Dasyscypha capitata. Mycologia 75: 423–435

Jaillard B (1987) Les structures rhizomorphes calcaires: modèle de réorganisation des minéraux du sol par les racines. Institut National de la Recherche Agronomique, Laboratoire de Science du Sol.

Johnston CG & Vestal JR (1993) Biogeochemistry of oxalate in the Antarctic cryptoendolithic Lichen-dominated community. Microb. Ecol. 25: 305–319

Kahle CF (1977) Origin of subaerial Holocene calcareous crust: Role of algae, fungi, and sparmicritization. Sedimentology 24: 413–435

Klappa CF (1979) Calcified filaments on Quaternary calcretes: Organomineral interaction in the subaerial vadose environment. J. Sedim. Petrol. 49: 955–968

Krumbein WE (1968) Geomicrobiology and geochemistry of lime crusts in Israel. In: Müller G & Friedman GM (Eds) Recent Developments in Carbonate Sedimentology in Central Europe (pp 138–147). Springer, Heidelberg

Krumbein WE, Petersen K & Schellnhuber HJ (1989) On the geomicrobiology of yellow, orange, red, brown and black films and crusts developing on several different types of stone and objects of art. In: Proc. Int. Symp. Le pellicole da ossalati: origine e significato nella conservazione delle opere d'arte (pp 337–351). Centro C.N.R. Gino Bozza, Milano

Lapeyrie F, Picatto C, Gerard J & Dexheimer J (1990) T.E.M. study of intracellular and extracellular calcium oxalate accumulation by ectomycorrhizal fungi in pure culture or in association with Eucalyptus seedlings. Symbiosis 9: 163–166

Leavens PB (1968) New data on whewellite. Am. Mineral. 53: 455–463

Malajczuk BN & Cromack K (1982) Accumulation of calcium oxalate in the mantle of ectomycorrhizal roots of Pinus radiata and Eucalyptus marginata. New Phytol. 92: 527–531

Monger HC, Daugherty LA & Gile LH (1991) A microscopic examination of pedogenic calcite in an aridisol of Southern New Mexico. In: Occurrence, Characteristics and Genesis of Carbonate, Gypsum and Silica Accumulations in Soils (pp 37–60). Soil Sci. Soc. Amer. Spec. Publ. no 26

Moore CH (1989) Carbonate Diagenesis and Porosity. Develop. in Sediment. no 46. Elsevier, Amsterdam

Phillips SE, Milnes AR & Foster RC (1987) Calcified filaments: An example of biological influences in the formation of calcrete in South Australia. Aust. J. Soil Res. 25: 405–428

Robert M & Berthelin J (1986) Role of biological and biochemical factors in soil mineral weathering. In: Interactions of Soil Minerals with Natural Organics and Microbes (pp 453–495). Soil Sci. Soc. Amer. Spec. Publ. no 17

Roques H (1964) Contribution à l'étude statique et cinétique des systèmes gaz carbonique – eau – carbonate. Annales de Spéléologie 19: 255–486

Roques H (1975) Chimie des carbonates et hydrogéologie karstique. Phénomènes karstiques I, C.E.R.C.G.-C.N.R.S. 2nd ed., Paris

Schlegel HS (1986) General Microbiology. Cambridge Univ. Press 6th ed., Cambridge

Steinen P (1974) Phreatic and vadose diagenetic modification of Pleistocene limestone: Petrographic observations from the subsurface of Barbados, West Indies. American Association of Petroleum Geologists Bull. 58: 1008–1024

Torre de la AM, Gomez-Alarcon G, Vizcaino C & Teresa Garcia M (1993) Biochemical mechanisms of stone alteration carried out by filamentous fungi living in monuments. Biogeochemistry 19: 129–147

Verrecchia EP (1992) Le rôle de la sédimentation, de l'activité biologique et de la diagénèse dans l'édification des nari-calcretes de Nazareth (Galilée, Israël). Mém. Sci. Terre, Université P. et M. Curie, n° 92–17, 2 vol

Verrecchia EP & Verrecchia KE (1994) Needle-fiber calcite: A critical review and a proposed classification. J. Sedim. Res. A64: 650–664

Verrecchia EP, Dumont JL & Verrecchia KE (1993) Role of calcium oxalate biomineralization by fungi in the formation of calcretes: A case study from Nazareth, Israel. J. Sedim. Petrol. 63: 1000–1006

Wadsten T & Moberg R (1985) Calcium oxalate hydrates on the surface of lichens. Lichenologist 17: 239–245

Webley DM, Henderson EK & Taylor F (1963) The microbiology of rocks and weathered stones. J. Soil Sci. 14: 102–112

Wollast R (1971) Kinetic aspects of the nucleation and growth of calcite from aqueous solutions In: Bricker PO (Ed) Carbonate Cements (pp 274–277). John Hopkins Univ., Stud. in Geology, 19

Wright VP (1989) Terrestrial stromatolites and laminar calcretes: A review. Sedim. Geol 65: 1–13

Yaalon DH & Singer S (1974) Vertical variation in strength and porosity of calcrete (nari) on chalk, Shefela, Israel and interpretation of its origin. J. Sedim. Petrol. 44: 1016–1023

Appendix

Calculation of the total balance during the transformation of calcium oxalate into carbonate (Eqn 10)

Two cases are considered in which the pH is lower or higher than 8.3. If pH <8.3, $|CO_3^{2-}|$ is negligible compared to $|CO_2|$ and $|CO_3H^-|$, and if pH >8.3, $|CO_2|$ is negligible compared to $|CO_3H^-|$ and $|CO_3^{2-}|$. In each case, two steps are studied. In step $0 \rightarrow 1$, calcium oxalate is dissolved and transforms into carbonate. In step $1 \rightarrow 2$, precipitation of $CaCO_3$ occurs.

At pH <8.3, we have:

$$-\Delta(CaC_2O_4) = 2\Delta C_T \quad (1)$$

$$-\Delta(CaC_2O_4) = \Delta|Ca^{2+}| \quad (2)$$

$$\Delta|CO_3H^-| \approx 2\Delta|Ca^{2+}| \tag{3}$$

$$C_T \approx \Delta|CO_3H^-| + \Delta|CO_2| \tag{4}$$

During the step $0 \rightarrow 1$, there is dissolution of calcium oxalate, therefore $\Delta|Ca^{2+}| > 0$, leading to:

$$\Delta|Ca^{2+}| > 0 \Rightarrow -3\Delta|Ca^{2+}|_{0\rightarrow 1} \approx 2\Delta|CO_2|_{0\rightarrow 1} \Rightarrow$$
$$\Delta|CO_2|_{0\rightarrow 1} < 0 \Rightarrow \Delta pH_{0\rightarrow 1} > 0 \tag{5}$$

On the figurative point 1 (Figure 7a), the solution begins to precipitate calcium carbonate on various substrates (e.g. micrite, bacteria or needle-fiber calcite on which it forms winglets), after having become supersaturated between states 0 and 1.

In step $1 \rightarrow 2$, there is precipitation of $CaCO_3$. We have:

$$\Delta C_T = \Delta|Ca^{2+}| \tag{6}$$

$$\Delta C_T \approx \Delta|CO_3H^-| + \Delta|CO_2| \tag{7}$$

$$\Delta|CO_3H^-| \approx 2\Delta|Ca^{2+}| \tag{8}$$

(6), (7), and (8) yield:

$$\Delta|CO_2| + \frac{\Delta|CO_3H^-|}{2} \approx 0 \tag{9}$$

$$\Rightarrow \Delta|CO_2|_{1\rightarrow 2} = -\Delta|Ca^{2+}|_{1\rightarrow 2} \tag{10}$$

Because there is precipitation of $CaCO_3$, $\Delta|Ca^{2+}|_{1\rightarrow 2} < 0 \Rightarrow \Delta|CO_2|_{1\rightarrow 2} > 0 \Rightarrow \Delta pH_{1\rightarrow 2} < 0$. Equations (5) and (10) give the slope of the two reactions (in step $0 \rightarrow 1$ and step $1 \rightarrow 2$) on a $|CO_2| = f(|Ca^{2+}|)$ plot (Figure 7b). In step $0 \rightarrow 1$, the slope is $\frac{-3}{2}$, and in step $1 \rightarrow 2$, its value is -1.

A pH >8.3 leads to similar conclusions because $|CO_2|$ is negligible compared to $|CO_3H^-|$ and $|CO_3^{2-}|$. Therefore, we have $\Delta|CO_3^{2-}|_{0\rightarrow 1} \approx \frac{3}{2}\Delta|Ca^{2+}|_{0\rightarrow 1}$ and $\Delta|CO_3^{2-}|_{1\rightarrow 2} \approx \Delta|Ca^{2+}|_{1\rightarrow 2}$ with $|CO_3^{2-}|_{aq} = \frac{\pi}{|Ca^{2+}|_{aq}}$ (Figure 7a but with pH >8.3, and Figure 8).

In conclusion, after becoming supersaturated during the transformation of CaC_2O_4 into $CaCO_3$ by solubilization, the solution is less concentrated at the final state 2 than at the initial state 0. This result is true whatever the pH but at pH = 8.3, $|CO_2| = |CO_3^{2-}|$ states 0 and 2 being interchangeable. Then during the $|Ca^{2+}|_{0\rightarrow 2}$ variation, $\Delta|Ca^{2+}|$ goes through a minimum value at pH 8.3. Therefore, $|Ca^{2+}|_2 - |Ca^{2+}|_0 \leq 0$.

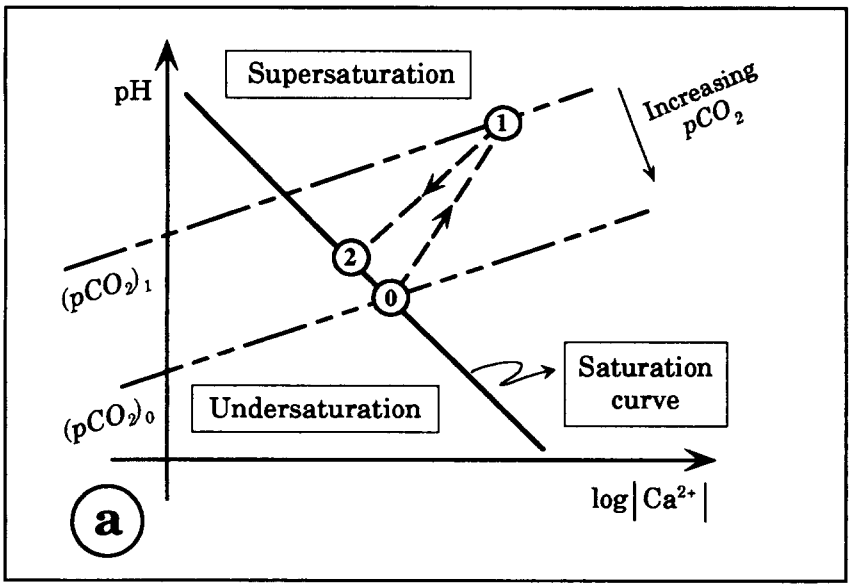

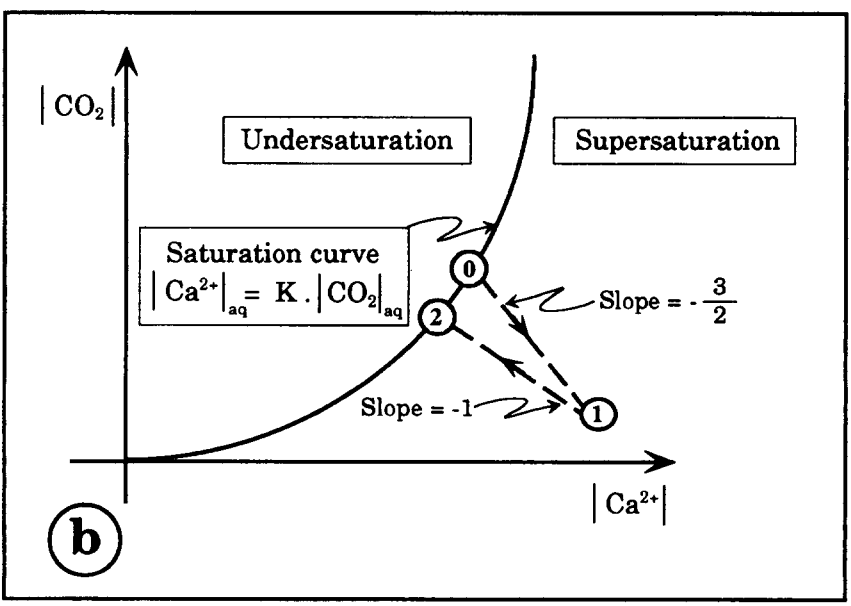

Figure 7. a. Graph pH = f(log |Ca^{2+}|) showing the evolution of the solution when the pH <8.3. b. Graph illustrating the two slope values of |CO_2| = f(|Ca^{2+}|) during the total transformation (steps 0 to 1 then 1 to 2).

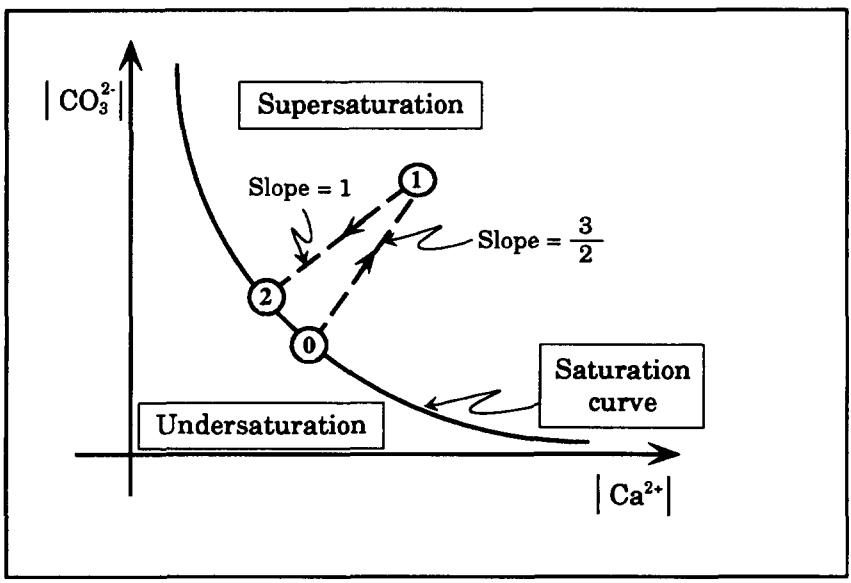

Figure 8. Graph illustrating the two slope values of $|CO_3^{2-}| = f(|Ca^{2+}|)$ during the total trans formation (steps 0 to 1 then 1 to 2).